© creative

Scientific paper

Cyclopentyl-linked N-Acylthioureas as Promising Urease Inhibitors: Insights from *in vitro* Bioassay, Structure-activity Relationships and Computational Analysis

Khansa Mumtaz, Sumera Zaib, Amer Saeed, Atteeque Ahmed, Afifa Tur Rehman, Aneeza Asghar, and Imtiaz Khan

¹ Department of Chemistry, Quaid-i-Azam University, Islamabad 45320, Pakistan

² Department of Basic and Applied Chemistry, Faculty of Science and Technology, University of Central Punjab, Lahore 54590, Pakistan

³ Manchester Institute of Biotechnology, The University of Manchester, 131 Princess Street, Manchester M1 7DN, United Kingdom

* Corresponding author: E-mail: asaeed@qau.edu.pk (A.S.); sumera.zaib@ucp.edu.pk (S.Z.)

Received: 08-18-2025

Abstract

Helicobacter pylori is a Gram-negative bacteria responsible for gastrointestinal disorders, including chronic gastritis and potentially life-threatening conditions like gastric cancer. To manage these adverse outcomes, inhibiting the urease enzyme emerges as a promising strategy. A concise set of cyclopentyl-bearing N-acylthioureas $\bf 4a-j$ was synthesized, characterized and assessed for their ability to inhibit urease enzyme. All the tested compounds exhibited urease inhibitory activities, displaying superior enzyme inhibition when compared to the standard, thiourea (IC₅₀ values 23.00 ± 0.03 μM). $\bf 4a$ and $\bf 4b$ exhibited the highest inhibitory efficacy with IC₅₀ values of 2.21 ± 0.62 and 3.92 ± 0.59 μM, respectively. Both compounds demonstrated ≈10- and ≈6-folds superior inhibition than standard inhibitor, respectively. Moreover, molecular docking investigations revealed crucial interactions between potent ligands and active site residues. Molecular dynamics simulations and ADME properties revealed ligand-protein stability and druglikeness behavior of potent leads paving the way for treatment for gastritis.

Keywords: Acylthioureas; gastritis; mixed inhibition; pharmacokinetic properties; structure-activity relationship; ure-ase.

1. Introduction

Enzymes are highly specialized biocatalytic proteins in living cells. They exhibit remarkable selectivity, strong affinity for their substrates, and exceptional catalytic efficiency. Enzymes play a vital role in facilitating a wide range of chemical transformations that are essential for sustaining life and accelerating various biochemical processes within the body. These unique attributes of enzymes make them perfect target to control various physiological processes. Because of this potential, enzymes find extensive medical applications, either independently or in conjunction with other treatments, for the safe management of a wide range of diseases. In the treatment of diseases resulting from enzyme-related disorders, enzyme inhibitors are considered as a promising strategy. Inhibitors are substanc-

es that can interfere with enzymatic activity by attaching themselves to the enzyme's active site, either in a reversible or irreversible manner. This binding obstructs the enzyme's active site and blocks the enzymatic reaction it catalyzes.³ Urease is an enzyme found in a variety of microorganisms, including bacteria, fungi, plants, and algae. It has the remarkable ability to rapidly catalyze the breakdown of urea into ammonia and carbon dioxide. When ammonia levels rise due to this enzymatic activity, it significantly boosts the activity of Helicobacter pylori, leading to damage to the stomach lining, infections in the stomach and duodenum, the development of peptic ulcers, and even an increased risk of gastric cancer. Controlling infectious diseases caused by H. pylori can be partially achieved by inhibiting the activity of urease through the use of urease inhibitors.⁵ Within the urease enzyme's active site, there are two nickel at-

oms coordinated with hydroxide ions and three molecules of water. The urea molecule, acting as the enzyme's substrate, engages in weak hydrogen bond interactions with the enzyme, leading to the breakdown of urea into ammonia and carbonic acid.⁶ Due to the specific structure of the urease binding site, there has been significant interest from the scientific community in devising strategies for designing urease inhibitors. This approach holds promise as an effective therapeutic option against diseases caused by pathogenic microorganisms dependent on urease, and it has garnered increased attention in recent years.7 Around half of the world's population is carrying an H. pylori infection. This species of bacteria can exist in the stomach of infected individuals for their entire lives without triggering any symptoms. The widespread presence of H. pylori in humans suggests that this microorganism has evolved mechanisms to resist the body's immune defenses.8 H. pylori is a microaerophilic bacterium classified as Gram-negative. It exhibits a preference for inhabiting the surface of epithelial cells within the human gastric mucosa, as well as the lowermost layer of the gastric mucus.9 In recent times, antibiotic-resistant variants have surfaced on a global scale, posing a significant challenge due to the limited availability of alternative treatments. It has been noted that the absence of urease activity results in the bacterium's inability to establish colonization. 10 The extensive utilization of antibiotics has led to the proliferation of antimicrobial resistance, consequently leading to decreased rates of successful eradication. 11 Urease plays crucial roles in H. pylori's ability to survive, colonize, and cause disease in the challenging acidic conditions of the stomach. It significantly contributes to the bacterium's ability to persist in the host's body during infection. Consequently, urease is regarded as one of the most potent and optimistic targets for the development of antibacterial compounds to combat this pathogen.¹²

Acylthioureas are comprised of thiourea with *N*-acyl substitution. Their holographic diagram, polarity profile and hydrogen bond donor acceptor nature make them pharmaceutically versatile core structure in various marketed drugs and therapeutically active compounds. 13 Additionally, they serve as precursors for ubiquitously distributed heterocyclic families in pharmaceutical chemistry. Moreover, they ligate with various transition metal ions to form complexes. These structural motifs possess huge therapeutic potential and attract the attention of synthetic medicinal chemists.¹⁴ Acylthioureas have become appealing alternatives in a variety of fields, such as ion sensing, corrosion inhibition, and find uses in molecular electronics and metal extraction procedures. The numerous biological activities displayed by thiourea derivatives have long attracted the interest of medicinal chemists. 15 These compounds have a wide range of biological activities, such as antibacterial and anti-inflammatory capabilities, 16-18 antimalarial activity, 19 and potency against tuberculosis. 20 As we endure in our mission to gather information about the structural characteristics and numerous applications of 1-acyl-3-cyclopentyl thiourea analogs, ongoing progress has motivated us to offer a comprehensive overview

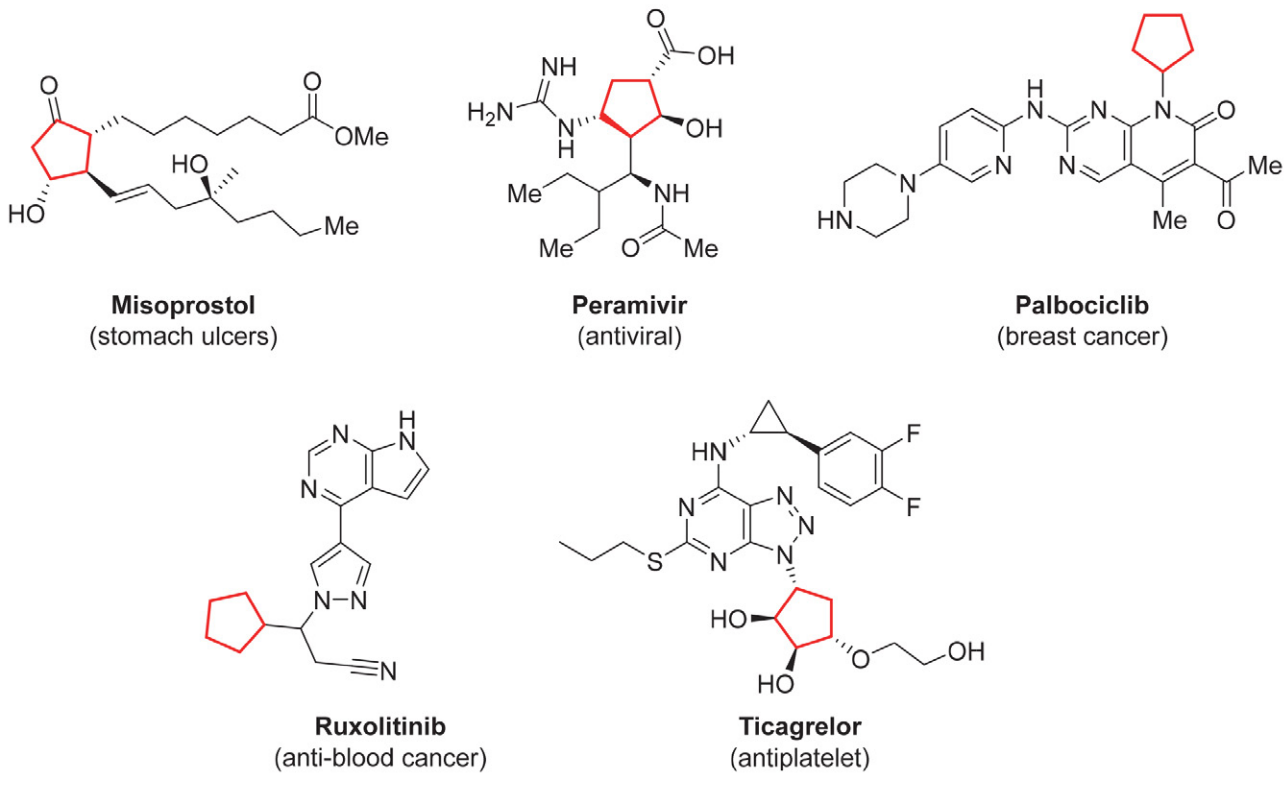


Figure 1. Therapeutically active cyclopentyl incorporated drugs.

to shed light on the exciting developments within the family of these compounds.

In parallel, a fused cyclopentane ring is an essential part of the steroidal architecture in all steroid-based treatments. The backbone of the most prostaglandins is cyclopentane.²¹ The most recent prostaglandin analogue is latanoprostene²² from Baush and Lomb, which is used to treat ocular hypertension. Neuraminidase inhibitor paramivir²³ is used in the treatment of influenza. Breast cancer is curable with palbociclib²⁴, a drug made by Pfizer. In order to cure bone marrow cancer, ruxolitinib²⁵ is employed (Figure 1).

In view of the literature findings, this works report the synthesis of a concise library of cyclopentyl linked N-acyl thioureas for the efficient inhibition of urease enzyme. In vitro assay results revealed remarkable potential with low IC_{50} values. The diversity of substituents allowed us to conclude various impactful structure-activity relationships. Computational analysis revealed the formation of viable binding interactions between the potent ligands and the active site amino acid residues whereas ADME prediction favored the druglikeness profile of potent compounds.

2. Materials and Methods

2. 1. Experimental

Analytical grade reagents and chemicals were employed without further purification. Solvent purification and drying were carried out using standard protocols. The R_f values were determined using pre-coated silica gel plates Kiesel 60 F₂₅₄ by observing under the UV. Melting points were determined by using Stuart SMP3 digital melting point apparatus in open-end capillaries. ¹H and ¹³C NMR spectra were recorded on Bruker 300/600 MHz and 75/150 MHz spectrophotometer, respectively, using DMSO as a solvent.

2. 2. General Method for the Synthesis of Cyclopentyl-linked N-Acylthioureas 4a-j

The substituted benzoic acids **1a-j** (4 mmol) were converted into acid chlorides by reacting with thionyl chloride (4.91 mmol) in the presence of catalytic amount of DMF under reflux condition for 3 h. The synthesized acid chlorides were dissolved in the acetone (5 mL) and drop-wise added to the potassium thiocyanate (4 mmol) solution in acetone (10 mL). The mixture was refluxed for 1.5 h under inert conditions. The cyclopentylamine (**3**) (4 mmol) was dissolved in dry acetone (3 mL) and added into the reaction mixture and refluxed for 3 h. After completion of reaction, monitored by TLC, the reaction mixture was decanted onto crushed ice. The precipitated products were filtered off, washed with water and recrystallized from ethanol to furnish compounds **4a-j**.

2. 3. Characterization Data of Compounds 4a-i

2. 3. 1. *N*-(Cyclopentylcarbamothioyl)benzamide (4a)

$$\bigcup_{N} \bigcup_{H} \bigcup_{N} \bigcup_{N$$

Light yellow crystals; yield: 91% (0.93 g); m.p: 132–135 °C; R_f : 0.50 (20% EtOAc in n-hexane); ¹H NMR (300 MHz, DMSO- d_6) δ (ppm): 11.3 (s, 1H, NH), 10.96 (d, 1H, NH), 7.92 (dd, J = 1.2, 2H, ArH), 7.66–7.60 (m, 1H, ArH), 7.53–7.48 (m, 2H, ArH), 4.61–4.52 (quintet, J = 6.3 Hz, 1H, CH), 2.00–1.54 (m, 8H, cy); ¹³C NMR (75 MHz, DMSO- d_6) δ (ppm): 179.8, 168.8, 133.4, 132.6, 128.9, 127.8, 56.68, 32.2, 23.8; Anal. calcd. for $C_{13}H_{16}N_2OS$: C, 62.87; H, 6.49; N, 11.28; S, 12.91%; found: C, 62.85; H, 6.48; N, 11.25; S, 12.87%.

$$\bigcup_{\mathsf{Me}}^{\mathsf{O}} \bigcup_{\mathsf{H}}^{\mathsf{S}} \bigcup_{\mathsf{H}}^{\mathsf{N}}$$

2. 3. 2. N-(Cyclopentylcarbamothioyl)-2methylbenzamide (4b)

Orange crystals; yield: 85% (0.92 g); m.p: 153–155 °C; R_f : 0.5 (20% EtOAc in n-hexane); 1 H NMR (300 MHz, DMSO- d_6) δ (ppm): 11.6 (s, 1H, NH), 10.60 (d, 1H, NH), 7.93–7.90 (m, 4H, ArH), 4.63–4.53 (quintet, J=6.9 Hz, 1H, C-H), 2.40 (s, 3H, CH₃), 2.10–1.54 (m, 8H, cy); 13 C NMR (75 MHz, DMSO- d_6) δ (ppm): 180.23, 173.8, 133.6, 134.6, 131.2, 131.0, 128.4, 125.9, 56.68, 32.2, 23.8, 20.23; Anal. calcd. for C₁₄H₁₈N₂OS: C, 64.09; H, 6.91; N, 10.68; S, 12.22%; found: C,64.04; H, 6.92; N,10.69; S, 12.21%.

2. 3. 3. 2-Chloro-*N*-(cyclopentylcarbamothioyl) benzamide (4c)

White solid; yield: 76% (0.85 g); m.p: 162–164 °C; R_f : 0.42 (n-hexane : ethyl acetate = 8:2); ¹H NMR (300 MHz, DMSO- d_6) δ (ppm): 11.73 (s, 1H, N-H), 10.67 (d, J = 7.2 Hz, 1H, N-H), 7.61–7.30 (m, 4H), 4.65–4.30 (m, 1H), 2.26–1.65 (m, 4H), 1.65–1.41 (m, 4H); ¹³C NMR (75 MHz, DMSO- d_6) δ (ppm): 179.5 (C, thiocarbonyl), 168.3 (C, amide), 134.8, 132.4, 130.3, 129.9, 129.6, 127.5, 56.6 (C1, Cy), 32.2, 23.8 (CH₂, Cy). Anal. Calcd. for C₁₃H1₅ClN₂OS:

C, 55.21; H, 5.35; Cl, 12.54; N, 9.91; S, 11.34; found: C, 55.18; H, 5.31; N, 9.89; S, 11.31.

2. 3. 4. N-(Cyclopentylcarbamothioyl)-2nitrobenzamide (4d)

Brown crystals; yield: 66% (0.71 g); m.p: 170–174 °C; R_f : 0.25 (n-hexane : ethyl acetate = 8:2); 1 H NMR (300 MHz, DMSO- d_6) δ (ppm): 12.20 (s, 1H, N-H), 11.87 (s, 4H, N-H), 10.56 (d, J = 7.3 Hz, 4H), 8.21 (dd, J = 10.7, 8.3 Hz, 6H), 7.93–7.84 (m, 6H), 7.80–7.67 (m, 12H), 4.55 (dt, J = 13.0, 6.7 Hz, 4H), 2.05 (dd, J = 13.3, 8.3 Hz, 8H), 1.99–1.25 (m, 27H). 13 C NMR (75 MHz, DMSO- d_6) δ (ppm): 179.4 (C, thiocarbonyl), 168.0 (C, amide), 166.9, 145.9, 145.7, 135.2, 135.0, 132.0, 131.7, 131.0, 129.8, 128.9, 124.6, 124.6, 56.6 (C1, Cy), 32.2, 23.8. Anal. Calcd. for $C_{13}H_{15}N_3O_3$ S: C, 53.23; H, 5.15; N, 14.32; S, 10.93; found: C, 53.19; H, 5.10; N, 14.29, S, 10.91.

2. 3. 5. *N*-(Cyclopentylcarbamothioyl)-3,5-dimethoxybenzamide (4e)

Orange solid; yield: 87% (1.1 g); m.p: 105-108 °C; R_f : 0.5 (n-hexane : ethyl acetate = 8:2); 1 H NMR (300 MHz, DMSO- d_6) δ (ppm): 10.9 (s, 1H, N-H), 10.12–10.09 (d, 1H, N-H), 7.15–7.14 (d, J = 3.1 Hz, 2H, Ar-H), 6.73–6.75 (m, 1H, Ar-H), 4.52–4.61 (quintet, J = 6.4 Hz, 1H, C-H), 3.8 (s, 6H, OCH₃), 1.54–2.0 (m, 8H, cy); 13 C NMR (75 MHz, DMSO- d_6) δ (ppm): 179.23 (C, thiocarbonyl), 167.8 (C, amide), 161.4, 134.4, 105.6, 104.1 (aromatic carbons), 56.7 (C1, Cy), 32.2, 23.8 (cyclopentyl carbons), 55.23 (C, methyl). Anal. Calcd. for C₁₅H₂₀N₂O₃S: C, 58.42; H, 6.54; N, 9.08; S, 10.40; found: C, 58.41; H, 6.50; N, 9.05; S, 10.38.

2. 3. 6. N-(Cyclopentylcarbamothioyl)-3,4-dimethoxybenzamide (4f)

Yellow crystals; yield: 86% (1.1 g); m.p: 110–114 °C; R_f : 0.35 (*n*-hexane : ethyl acetate = 8:2); ¹H NMR (300 MHz, DMSO- d_6) δ (ppm): 11.25–11.01 (m, 4H, N-H),

7.70–7.53 (m, 4H, N-H), 7.07 (d, J = 8.6 Hz, 2H), 4.70–4.32 (m, 2H), 3.84 (s, 12H), 2.19–1.99 (m, 3H), 1.61 (ddd, J = 14.4, 10.7, 5.2 Hz, 14H); ¹³C NMR (75 MHz, DMSO- d_6) δ (ppm): 179.9 (C, thiocarbonyl), 168.0 (C, amide), 153.29, 148.5, 124.2, 123.1, 111.8, 111.3, 56.6 (C1, Cy), 56.1, 56.0, 32.3, 23.8. Anal. Calcd. for C₁₅H₂₀N₂O₃S: C, 58.42; H, 6.54; N, 9.08; S, 10.40; found: C, 57.41; H, 6.32; N, 9.01; S, 10.37.

2. 3. 7. *N*-(Cyclopentylcarbamothioyl)-3,4,5-trimethoxybenzamide (4g)

White crystals; yield: 88% (1.22 g); m.p: 128–130 °C; R_f : 0.42 (n-hexane : ethyl acetate = 8:2); 1 H NMR (300 MHz, DMSO- d_6) δ (ppm): 11.34 (s, 1H, N-H), 11.09 (d, J = 7.2 Hz, 1H, N-H), 7.33 (s, 2H), 4.57 (dt, J = 12.3, 6.3 Hz, 1H), 3.86 (s, 6H), 3.74 (s, 3H), 2.29–1.76 (m, 2H), 1.76–1.31 (m, 6H); 13 C NMR (75 MHz, DMSO- d_6) δ (ppm): 179.8 (C, thiocarbonyl), 168.0 (C, amide), 152.9, 141.8, 127.2, 106.6, 60.5, 56.6 (C1, Cy), 56.5, 32.3, 23.8. Anal. Calcd. for $C_{16}H_{22}N_2O_4S$: C, 56.78; H, 6.55; N, 8.28; S, 9.47; found: C, 56.76; H, 6.49; N, 8.21; S, 9.44.

2. 3. 8. 4-Chloro-*N*-(cyclopentylcarbamothioyl) benzamide (4h)

White crystals; yield: 80% (0.92 g); m.p: 165-167 °C; R_f : 0.34 (n-hexane : ethyl acetate = 8:2); ${}^1\mathrm{H}$ NMR (300 MHz, DMSO- d_6) δ (ppm): 11.2 (s, 1H, N-H), 10.97–10.95 (d, 1H, N-H), 7.66–7.60 (d, 2H, Ar-H), 7.50–7.47 (d, J = 9.1Hz 2H, Ar-H), 4.63–4.51 (m, 1H, C-H), 1.54–2.0 (m, 8H, cy); ${}^{13}\mathrm{C}$ NMR (75 MHz, DMSO- d_6) δ (ppm): 180.83 (C, thiocarbonyl), 169.8 (C, amide), 136.1, 133.94, 129.6, 128.6 (aromatic carbons), 56.68 (C1, Cy), 32.2–23.8 (cyclopentyl carbons). Anal. Calcd. for $\mathrm{C}_{13}\mathrm{H}_{15}\mathrm{ClN}_2\mathrm{OS}$: C, 55.21; H, 5.35; N, 9.91S, 11.34; found: C, 55.17; H, 5.31; N, 9.89; S, 11.31.

2. 3. 9. *N*-(Cyclopentylcarbamothioyl)-1-naphthamide (4i)

White solid; yield: 70% (0.88 g); m.p: 195–197 °C; R_f : 0.5 (n-hexane : ethyl acetate = 8:2); 1 H NMR (300 MHz, DMSO- d_6) δ (ppm): 11.72 (s, 1H, N-H), 10.95 (d, J = 7.2 Hz, 1H, N-H), 8.07 (ddd, J = 9.3, 8.0, 2.1 Hz, 3H), 7.88–7.76 (m, 1H), 7.76–7.51 (m, 4H), 4.82–4.37 (m, 1H), 2.08 (d, J = 6.9 Hz, 2H), 1.67 (ddd, J = 10.2, 6.8, 6.0 Hz, 6H); 13 C NMR (75 MHz, DMSO- d_6) δ (ppm): 179.9 (C, thiocarbonyl), 170.5 (C, amide), 133.4, 131.9, 131.8, 129.9, 128.9, 127.8, 127.4, 126.9, 125.2, 125.1, 56.6, 32.3, 23.9. Anal.Calcd. for $C_{17}H_{18}N_2OS$: C, 68.42; H, 6.08; N, 9.39; S, 10.75; found: C, 68.39; H, 6.01; N,9.38; S,10.71.

2. 3. 10. 2,4-Dichloro-*N*-(cyclopentylcarbamothioyl)benzamide (4j)

White solid; yield: 70% (0.89 g); m.p: 180–183 °C; R_f : 0.45 (n-hexane : ethyl acetate = 8:2); 1 H NMR (300 MHz, DMSO- d_6) δ (ppm): 11.37 (s, 1H, N-H), 10.91–10.86 (d, 1H, N-H), 7.59–7.57 (m, 2H, Ar-H), 7.45 (d, J = 7.2 Hz, 1H, Ar-H), 4.61–4.52 (m, 1H, C-H), 1.53–2.1 (m, 8H, cy); 13 C NMR (75 MHz, DMSO- d_6) δ (ppm): 183.9 (C, thiocarbonyl), 168.2 (C, amide), 135.1–127.0 (aromatic carbons), 61.62 (C1, Cy), 32.9–24.1 (cyclopentyl carbons). Anal. Calcd. for $C_{13}H_{14}C_{12}N_2OS$: C, 49.22; H, 4.45; N, 8.83; S, 10.11; found: C, 48.99; H, 4.41; N, 8.81; S, 10.01.

2. 4. Inhibition Activity Assay

The evaluation of compounds **4a**–**j** for their inhibitory potential against urease was conducted through a slightly changed indophenol method. Thiourea served as positive control.²⁶⁻³⁰ In 96-well plate, reaction mixture was prepared by combining 40 µL of buffer solution (comprising 100 mM urea, 0.01 M K₂HPO₄, 1 mM EDTA, and 0.01 M LiCl₂, at pH 8.2) with 10 μL of jack bean urease enzyme (5 U/mL). Subsequently, the mixture was subjected to pre-incubation for a duration of 10 minutes at 37 °C. Later, 70 µL of phenolic reagent was used as coloring agent. Following incubation at 37 °C for 30 minutes, measurements were recorded at a wavelength of 630 nm using a plate reader (Bio-Tek ELx 800TM, USA). All the experiments were conducted in triplicate, and the outcomes were computed as percentage inhibition values. Compounds that demonstrated over 50% inhibition against urease underwent further evaluation through a series of 7-8 dilutions to determine their IC₅₀ values, utilizing Graph Pad PRISM (USA).

2. 5. Kinetics Studies

Michaelis-Menten kinetics experiments were utilized to identify the type of enzyme inhibition. Detailed

kinetics studies were conducted on the potent compound ${\bf 4a}$ to investigate the potential mechanism of action in inhibiting the enzyme. To achieve this, the initial rates of enzyme inhibition were measured at four substrate concentrations (25, 50, 100, 150 mM) both in the absence and presence of different concentrations of compound ${\bf 4a}$ (0, 1.105, 2.21, 3.315 μ M) against urease.³¹

2. 6. Docking Studies

The crystallographic structure of urease identified by its PDB ID: 3LA4 was retrieved from the RCSB PDB database, a resource for structural bioinformatics research.³² To prepare the receptor structure, water molecules and ligands were removed. The docking analysis was performed using AutoDock Vina, with initial method optimizations carried out.³³ PyRx tools were integrated with the docking software. Before starting the process, few steps were involved which included eliminating solvent molecules, adding hydrogen atoms, and computing charges. Additionally, default parameters were followed during the docking process by using AutoDock Vina.^{34,35} Finally, by using Discovery Studio Visualizer v4 and PyMOL, the interaction analysis for docked complexes was conducted.³⁶

2. 7. Molecular Dynamics Simulation

By using optimal docking pose of the complexes **4a** and **4b**, as determined by the docking results, molecular dynamics simulation was executed. The iMOD server (http://imods.chaconlab.org/) was employed for these MD simulations, with temperature held constant at 300 K and pressure maintained at 1 atm. The iMOD server provides an advanced method for conducting normal mode analysis (NMA) using internal coordinates, along with a user-friendly interface. This interface is optimized for compatibility with a wide range of modern web browsers and contemporary mobile devices, guaranteeing a smooth and efficient online experience.³⁷

2. 8. In silico ADME Properties

To evaluate the pharmacokinetic characteristics of compounds **4a** and **4b**, an online platform was utilized. SwissADME (http://www.swissadme.ch/index.php) served as the online tool for assessing the diverse properties of the compounds such as drug-like characteristics, solubility, and lead-like potential of the compounds. It was utilized to investigate various aspects of the compounds, including their physical and chemical properties, bioavailability, solubility, drug-likeness, lipophilicity, pharmacokinetics, and medicinal chemistry. The evaluation of these properties for compounds **4a** and **4b** was conducted to establish them as safer candidates for therapeutic use.³⁸

3. Results and Discussion

3. 1. Chemistry

A small library of cyclopentyl linked acylthioureas was synthesized according to the synthetic pathway outlined in scheme 1. In the first step, various substituted benzoic acids **1a–j** were converted into acid chlorides, which were then transformed to corresponding isothiocyanates **2a–j** in dry acetone. The *in situ* generated isothiocyanates were further reacted with cyclopentyl amine (3) to produce the desired thioureas **4a–j**.³⁹

Compound **4d**, featuring 2-NO₂ substitution on phenyl ring, showed moderate yield 66% as compared to other derivatives whereas compound **4a** with no substitution on phenyl ring displayed excellent yield 91%.

The synthesized compounds were fully characterized by various spectroscopic techniques. The synthesis of new cyclopentyl linked acylthiourea 4a was indicated in the FTIR spectra by the appearance of peaks at 3166 cm⁻¹, assigned to NH of thiourea. The peaks around 1668 cm⁻¹ (indicating presence of carbonyl functionality) and the absorption bands for aromatic system appeared at 1532 cm⁻¹. The C_{sp3}-H stretching of alkyl part appeared around 2961 cm⁻¹. ¹H NMR of **4a** further elucidated the structure. The spectrum of 4a revealed characteristic signals corresponding to different protons in the structure. Two individual singlets observed around 11.31 and 10.97 ppm were attributed to the NH protons of thiourea moiety. The aromatic region of the spectrum showed a set of multiplets ranging from 7.93-7.98 ppm, in agreement with the aromatic protons of phenyl group. The integration of these signals relates well with the predictable ratio, illustrating the correct determination of the structure. The quintet observed around 4.56 ppm was attributed to the methine proton of cyclopentyl adjacent to nitrogen. The two protons in the aliphatic region with integration of eight protons matched the expected ratio of four methylene of cyclopentyl. The chemical shift of this signal and coupling constants are in line with typical values of such protons, further confirming the presence of the cyclopentyl moiety in the structure.

The structure of target molecule **4a** was further confirmed with ¹³C NMR analysis. The signals resonating around 179.8 and 168.8 ppm correspond to C=S and C=O groups, respectively. The resonating signals in the range of 133.4 to 127.8 ppm were identified as the aromatic carbons present in the synthesized compounds. Additionally, three signals in the aliphatic region corresponding to cyclopentyl group provided further evidence of the formation of product. The NMR data allies well with the proposed target molecule and confirms successful formation of product **4a**. In conclusion, the H¹ and ¹³C NMR of the cyclopentyl linked acylthiourea **4a** validates the molecular structure and purity of the synthesized compound. All the remaining derivatives were characterized in the same way.

3. 2. *In vitro* Urease Inhibition and Structureactivity Relationship Analysis

A concise series of cyclopentyl linked N-acylthiourea derivatives 4a–j was synthesized and evaluated for their inhibitory potential against urease enzyme. Thiourea was employed as a standard (IC $_{50}$ 23.00 \pm 0.03 μ M). The IC $_{50}$ results are given in Table 1. The general structure of the synthesized compounds, shown in Figure 2, contains four different active moieties that could impact the biological outcome. Both hydrogen bond donor and acceptor sites are present that can facilitate the hydrogen bonding in the active site of urease enzyme. Cyclopentyl substituent can

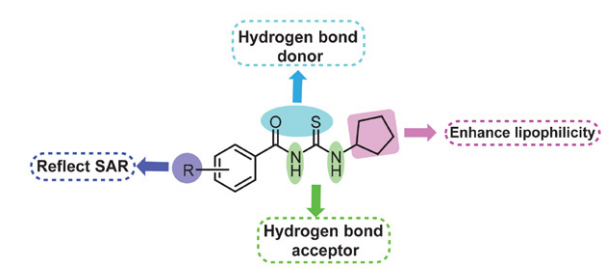


Figure 2. Active moieties in the target molecule are crucial for achieving potent biological activity.

Table 1. The inhibitory potential of compounds **4a**–**j** against urease.

Compoun		Jrease inhibition IC ₅₀ ± SEM (μM)
4a	O S N N N N N N N N N N N N N N N N N N	2.21 ± 0.62
4b	Me O S N N N N	3.92 ± 0.59
4c	CI O S N N N	13.49 ± 0.54
4d	NO ₂ O S N H H	5.80 ± 1.28
4e	MeO N N N N O O N N N N N N N N N N N N N	8.00 ± 0.87
4f	MeO N N N N N N N N N N N N N N N N N N N	9.71 ± 0.33
4g	MeO N N N N N N N N N N N N N N N N N N N	6.18 ± 0.57
4h	O S N N N	9.96 ± 0.41
4i	O S N	6.88 ± 0.49
4j	CI O S N N H H	9.26 ± 0.53
Thiourea	S H ₂ N NH ₂	23.00 ± 0.03

enhance the lipophilicity whereas the diverse substitutions at the phenyl ring of acyl component can play a crucial role in developing impactful structure-activity relationships, thus identifying the needful substituents for future drug discovery.

The range of inhibitory potential depicted by the tested derivatives was 2.21 to 13.49 µM, confirming that all the compounds were potent inhibitors against urease enzyme compared to standard, thiourea. The *in vitro* results revealed that compounds 4a and 4b show highest inhibition against urease, with IC₅₀ value of 2.21 \pm 0.62 μ M and $3.92 \pm 0.59 \mu M$, respectively (Figure 3). Compounds 4a and **4b** showed ≈10- and ≈6-folds superior inhibition than standard inhibitor, respectively. Compound 4a contains no additional substitution at phenyl ring whereas a methyl substituent was present at ortho-position of phenyl ring in **4b**. The replacement of methyl with a strong electron-withdrawing nitro group led to a slight decrease in inhibitory activity (4d; IC₅₀ 5.80 \pm 1.28 μ M), but still better than thiourea. However, the sudden decline was observed in inhibitory activity when chloro group was introduced at 2 and 4 positions of phenyl ring (4c; IC₅₀ 13.49 \pm 0.54 μ M) and (4h; IC₅₀ 9.96 \pm 0.41 μ M), respectively (Figure 4). When methoxy group was introduced at position 3 and 5 or at 3 and 4 of phenyl ring, similar level of reduction in inhibition potential was observed (4e; IC₅₀ 8.00 \pm 0.87 μ M) and (4f; IC₅₀ 9.71 \pm 0.33 μ M), however, when same group was added at position 3,4 and 5 of phenyl ring in compound 4g, slightly better inhibition profile was observed with IC₅₀ value of 6.18 \pm 0.57 μ M (Figure 5). The effective inhibitory potential like 4g was revealed when naphthyl group was introduced (4i; IC₅₀ 6.88 \pm 0.49 μ M). Overall, all the tested compounds showed superior inhibitory efficacy against urease enzyme compared to thiourea but with a varied degree of inhibition thus emphasizing the role of substituents on inhibition potential.

3. 3. Kinetics Studies

The mechanism of inhibition of most potent compound **4a** against urease was determined. By using Lineweaver–Burk graphs, enzyme inhibition mechanism and effect of inhibitor **4a** on $K_{\rm m}$ and V_{max} using reciprocal 1/S and 1/V were determined. The slope (K_m/V_{max}) of each line, in the Lineweaver–Burk plot was plotted *via* different concentrations of substrate and compound. Different concentrations such as 1.105, 2.21 and 3.315 μ M from 1 mM compound **4a** were used against urease enzyme. Compound **4a** (Figure 6) illustrates a mixed type of inhibition with apparent decrease in V_{max} as the concentration of inhibitor increases.

3. 4. Docking Studies

The most effective lead inhibitors, distinguished by their low IC_{50} values, were subjected to docking within the active site of urease (PDB: 4H9M). The lead compounds exhibited a binding affinity of -6.7 and -6.1 kcal/mol according to AutoDock Vina docking energies. These com-

IC₅₀ =
$$6.88 \pm 0.49 \,\mu\text{M}$$

Ph \rightarrow 2-Np decrease in inhibition

H \rightarrow Me \rightarrow NO₂ O S decrease in inhibition

 $4a$

IC₅₀ = $2.21 \pm 0.62 \,\mu\text{M}$

IC₅₀ = $3.92 \pm 0.59 \,\mu\text{M}$

IC₅₀ = $5.80 \pm 1.28 \,\mu\text{M}$

Figure 3. Structural variation from 4a to 4b, 4d and 4i showing decrease in urease inhibitory action.

Figure 4. Structural variation from 4c to 4h and 4j showing change in urease inhibitory action.



Figure 5. Structural variation from 4e to 4f and 4g showing change in urease inhibitory action.

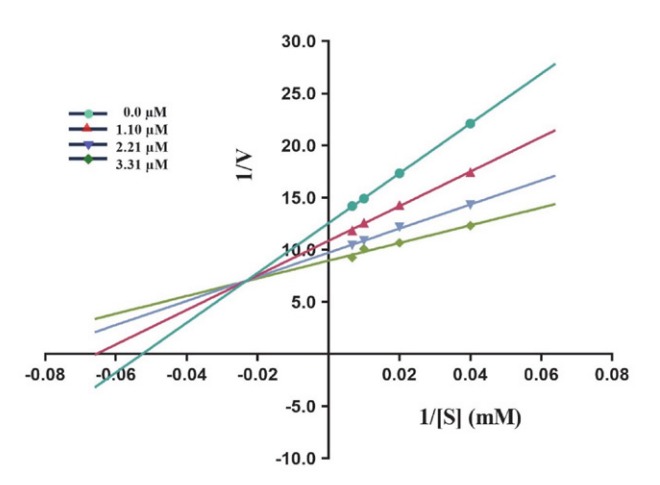


Figure 6. Mixed type of inhibition exhibited by compound **4a** against urease.

pounds displayed a variety of interactions with the amino acid residues located within the active site, as outlined in Table 2. Compounds 4a and 4b revealed interactions with various residues of amino acids such as Lys716, Phe712, Ala37, Thr33, Val36, Glu742 and Ser421. Compound 4a revealed alkyl interaction between carbon atom of cyclopentyl ring with 5.10 Å distance. Similarly, π -alkyl interactions were exhibited by carbon atoms of cyclopentane and benzamide rings with Phe712 (3.71 Å), Ala37 (5.21 Å) and Val36 (4.87 Å), respectively. Furthermore, π -sigma interaction was noticed between the carbon atom of benzamide ring and Thr33 with a distance of 3.76 Å. Moreover, Glu742 revealed π -anion interaction with carbon atom of benzamide ring with a distance of 4.31 Å. On the other hand, compound 4b showed hydrogen bond interaction between Glu742 and hydrogen atom at the distance of 2.96 Å. Additionally, hydrogen bond exhibited Tyr32 interactions

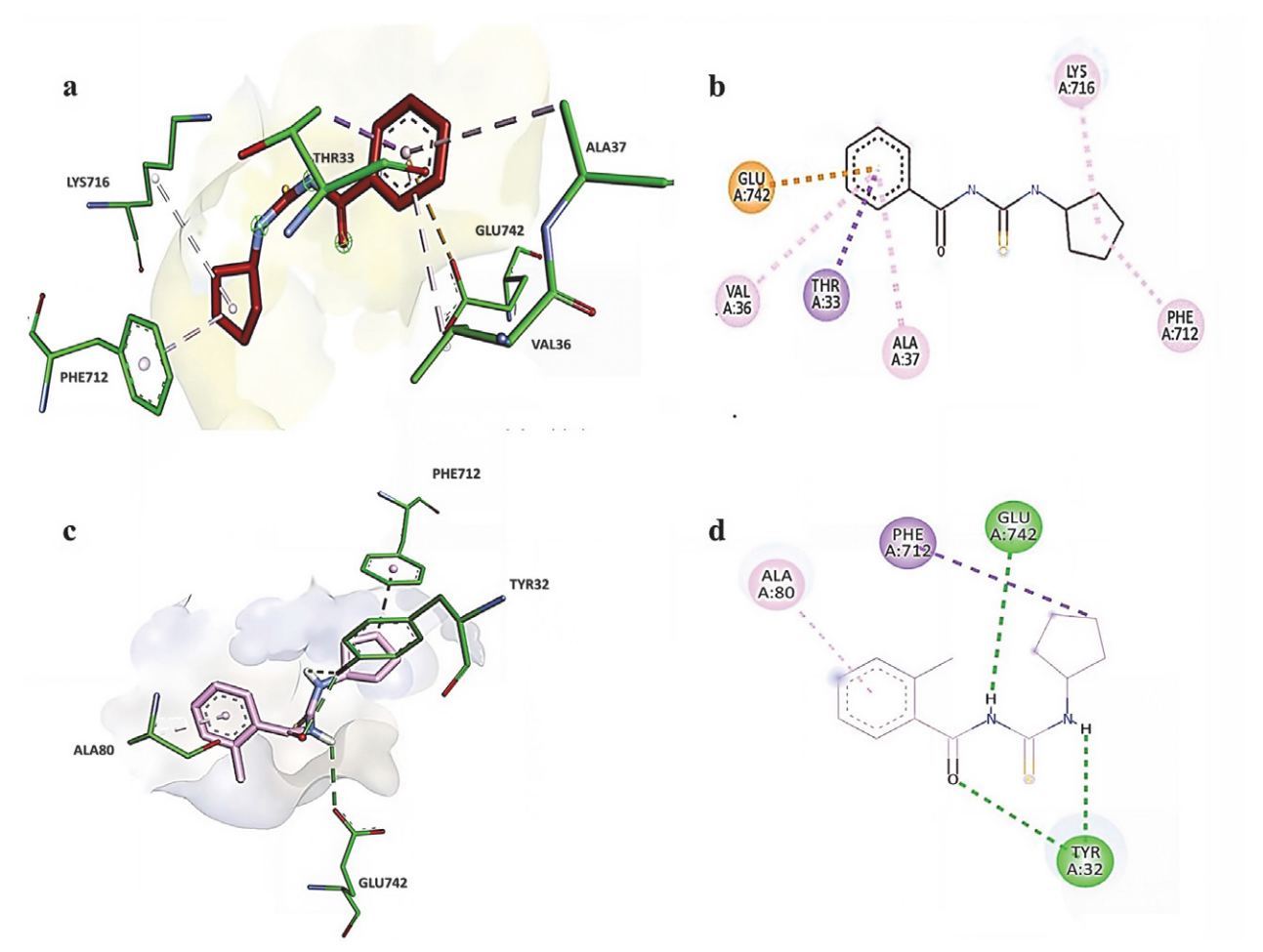


Figure 7. Illustration of 3D (a & c) and 2D (b & d) interactions of compounds 4a and 4b with urease. Green sticks represent the amino acid residues while red and pink sticks show the ligand.

with oxygen and hydrogen atom with the distance of 2.96 and 2.77 Å, respectively. However, π -sigma interaction was demonstrated between Phe712 and carbon atom of cyclopentyl ring at a distance of 3.51 Å. Furthermore, π -alkyl interaction was exhibited between Ala80 and carbon atom of benzamide ring, as shown in Figure 7.

Table 2. The binding interactions between receptor residues and compounds ${\bf 4a}$ and ${\bf 4b}$.

Com- pounds	Interacting amino acid residues	Interaction types	Distance (Å)
4a	Lys	Alkyl	5.10
	Phe	π-alkyl	3.71
	Ala	π-alkyl	5.21
	Thr	π-sigma	3.76
	Val	π-alkyl	4.87
	Glu	π -anion	4.31
4b	Glu	Hydrogen bond	2.96
	Tyr	Hydrogen bond	2.77
	Tyr	Hydrogen bond	2.96
	Phe	π-sigma	3.51
	Ala	π-alkyl	4.33

3. 5. Molecular Dynamics Simulations

To perform the molecular dynamics simulations, the iMOD server was used with the objective of evaluating the stability of the complex formed between the ligand and the protein. The results of the molecular dynamics simulations conducted for 4a are illustrated in Figure 8. Within Figure 8a, the varied levels of peaks correspond to different degrees of deformability, with lower peaks indicating decreased deformability, and higher peaks signifying increased deformability. On the other hand, Figure 8b illustrates that the eigenvalue exhibits an inverse correlation with the energy necessary for inducing structural deformation. Moreover, in Figure 8c, the covariance is visually denoted using three distinct colors: red denotes correlation, blue represents non-correlation, and white signifies anti-correlation. Transitioning to Figure 8d, the visualization of the elastic model network reveals the creation of springs. The degree of spring formation is indicated by the gray shade, with a significant portion of atoms taking part in spring formation.

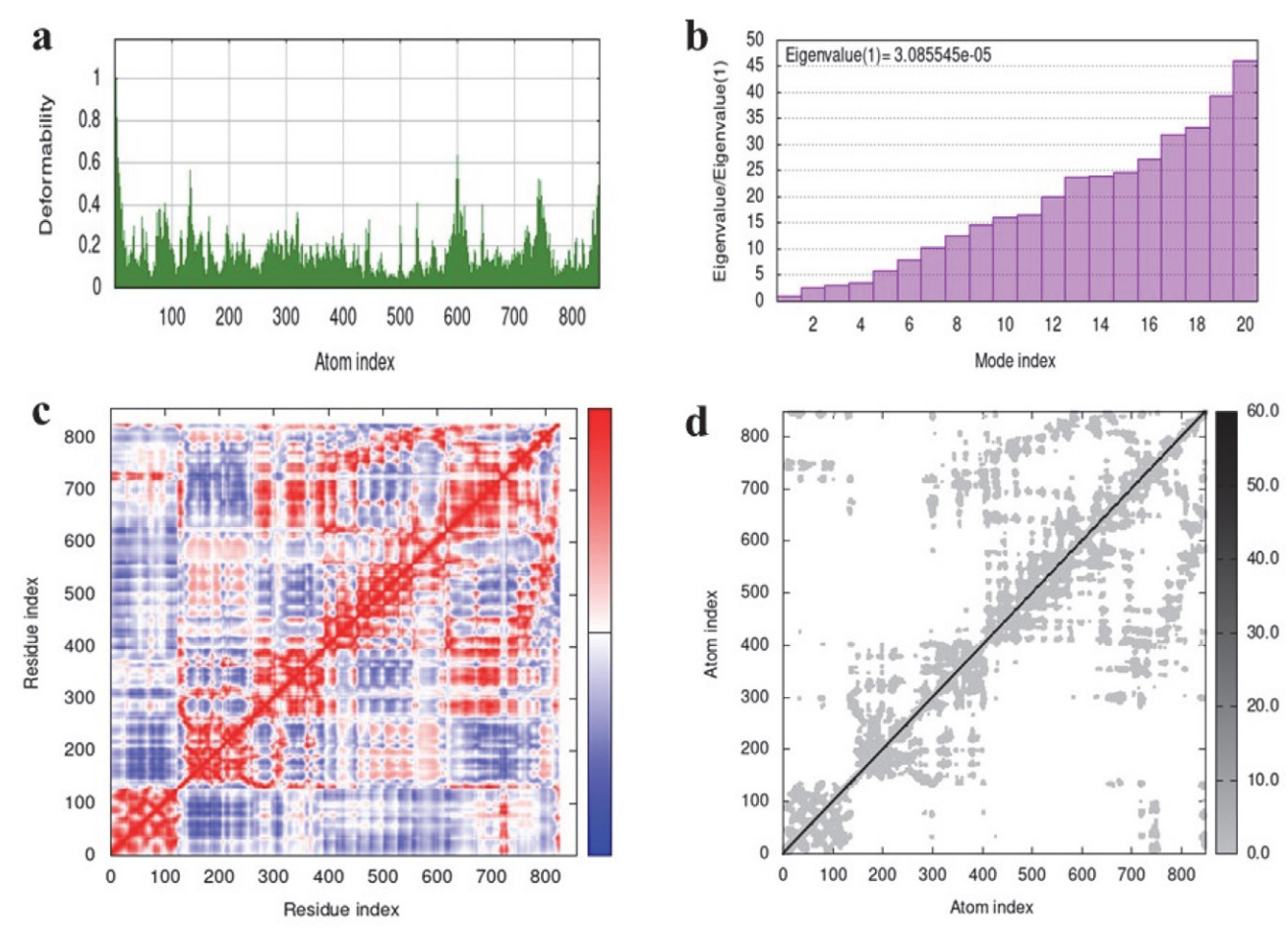


Figure 8. Molecular dynamics simulation of 4a by iMODs.

3. 6. ADME Analysis

The molecular weights of compounds 4a (248.34 g/ mol) and 4b (262.37 g/mol) fall within the acceptable range for orally active drugs (<500 g/mol), according to Lipinski's rule of five. Their molar refractivity values of 71.95 (4a) and 76.92 (4b) m³·mol⁻¹ indicate good molecular polarizability and topological polar surface area (TP-SA) values of 73.22 Å^2 for **4a** and 72.22 Å^2 for **4b** suggest efficient membrane permeability, as compounds with TP-SA values below 140 Å² are generally favorable. Additionally, their consensus log P values of 2.64 (4a) and 2.95 (4b) indicate moderate lipophilicity. Both compounds exhibit good solubility, high gastrointestinal (GI) absorption and potential to cross the membrane of nervous system. Furthermore, neither compound acts as a substrate for P-glycoprotein (P-gp), reducing the possibility of efflux-mediated drug resistance. Their predicted skin permeability (log K_p) values of -5.52 cm/s (4a) and -5.35 cm/s (4b) suggest transdermal absorption may be minimal. Additionally, no structural alerts were identified in the Pan-Assay Interference Compounds (PAINS) analysis predicting that substructures known to interfere with biological assays will not be formed as shown in Table 3.

Table 3. ADME analysis of compound 4a and 4b.

Characteristics	4a	4b
Formula	$C_{13}H_{16}N_2OS$	$C_{14}H_{18}N_2OS$
Molecular weight (gmol ⁻¹)	248.34	262.37
Molar refractivity (m ³ mol ⁻¹)	71.95	76.92
TPSA (Å ²)	73.22	72.22
Consensus $\log P_{o/w}$	2.64	2.95
Class	Soluble	Soluble
GI absorption	High	High
BBB permeant	Yes	Yes
P-gp substrate	No	No
CYP1A2 inhibitor	Yes	Yes
CYP2C19 inhibitor	Yes	Yes
CYP2C9 inhibitor	Yes	Yes
CYP2D6inhibitor	No	No
CYP3A4 inhibitor	No	No
$\log K_{\rm p}$ (skin permeation) (cm/s)	-5.52	-5.35
		Yes, 0 violation
Bioavailability score	0.55	0.55
PAINS	0 alert	0 alert
Synthetic accessibility	1.87	2.05

4. Conclusion

In summary, a concise library of cyclopentyl linked acyl thioureas was prepared in a facile fashion. The inhibitory effectiveness against urease was assessed using indophenol method. All these compounds demonstrated significantly superior inhibitory activity in comparison to the standard drug, thiourea. Remarkably, 4a and 4b appeared as the leading inhibitors, displaying exceptional effectiveness with an IC₅₀ value of 2.21 \pm 0.62 and 3.92 \pm 0.59 μ M, respectively. The docking studies showed various interactions occurring between complexes (4a, 4b) and the amino acids within the active site of urease. The primary inhibitor demonstrated significant docking score and favorable binding free energies, suggesting an effective binding interaction. In kinetics experiments, compound 4a revealed the mixed type of inhibition. The in silico AD-ME profile displayed a range of drug-like attributes for 4a and 4b.

Conflict of interest disclosure

The authors declare no conflict of interest financial or otherwise.

Acknowledgement

None.

Supplementary information

Supplementary data has been attached.

Funding

None.

CRediT authorship contribution statement

The authors declare their contribution as follows. Khansa Mumtaz: Investigation, Methodology, Formal analysis, Writing – review & editing original draft; Sumera Zaib: Conceptualization, Methodology, Resources, Writing – review & editing original draft, Supervision, Project administration; Aamer Saeed: Conceptualization, Methodology, Resources, Writing - review & editing original draft, Supervision, Project administration; Atteeque **Ahmed**: Investigation; **Afifa Tur Rehman**: Investigation, Methodology, Writing - review & editing original draft; Aneeza Asghar: Investigation, Methodology, Writing – review & editing original draft; Imtiaz Khan: Conceptualization, Methodology, Writing - review & editing original draft. All authors have read and agreed to the published version of the manuscript.

5. References

1. A. Kunamneni, C. Ogaugwu, D. Goli, in: C. S. Nunes, V. Kumar (Ed.): Enzymes in Human and Animal Nutrition, Academic Press, 2018, pp. 301-312.

DOI: 10.1016/B978-0-12-805419-2.00015-0

- 2. F. Michailidou, Angew. Chem. 2023, 135, e202308814. DOI: 10.1002/anie.202308814
- 3. G. Mohiuddin, K. M. Khan, U. Salar, M. A. Lodhi, A. Wadood, M. Riaz, S. Perveen, Bioorg. Chem. 2019, 83, 29-46. DOI: 10.1016/j.bioorg.2018.10.021
- 4. W. Yang, Q. Feng, Z. Peng, G. Wang, Eur. J. Med. Chem. 2022, 234, 114273. DOI: 10.1016/j.ejmech.2022.114273
- 5. S. A. A. S. Tirmazi, M. A. Qadir, M. Ahmed, M. Imran, R. Hussain, M. Sharif, M. Yousaf, M. Muddassar, J. Mol. Struct. 2021, 1235, 130226. DOI: 10.1016/j.molstruc.2021.130226
- 6. A. Ibrar, I. Khan, N. Abbas, Arch. Pharm. 2013, 346, 423-446. **DOI:** 10.1002/ardp.201300041
- 7. F. M. Oliveira, L. C. Barbosa, F. M. Ismail, RSC Adv. 2014, 4, 18998-19012. DOI: 10.1039/C4RA01454E
- 8. Y. F. Rego, M. P. Queiroz, T. O. Brito, P. G. Carvalho, V. T. de Queiroz, A. de Fátima, F. Macedo Jr, J. Adv. Res. 2018, 13, 69–100. **DOI:** 10.1016/j.jare.2018.05.003
- 9. S. Xiao, K. Shang, W. Li, X. Wang, Sens. Actuators B. Chem. **2022**, *355*, 131284. **DOI**: 10.1016/j.snb.2021.131284
- 10. M. Imran, S. Waqar, K. Ogata, M. Ahmed, Z. Noreen, S. Javed, N. Bibi, H. Bokhari, A. Amjad, M. Muddassar, RSC Adv. 2020, 10, 16061-16070. DOI: 10.1039/D0RA02363A
- 11. M. A. Siddiqui, O. Sadiq, U. Iqbal, O. Siddique, S. M. Jafri, M. Blumenkehl, Gastroenterology. 2017, 152, S951. DOI: 10.1016/S0016-5085(17)33235-3
- 12. L. V. Modolo, A. X. de Souza, L. P. Horta, D. P. Araujo, A. de Fátima, J. Adv. Res. 2015, 6, 35-44. DOI: 10.1016/j.jare.2014.09.001
- 13. A. Saeed, U. Flörke, M. F. Erben, J. Sulphur Chem. 2014, 35, 318-355. DOI: 10.1080/17415993.2013.834904
- 14. U. Zahra, A. Saeed, T. A. Fattah, U. Flörke, M. F. Erben, RSC *Adv.* **2022**, *12*, 12710–12745. **DOI:** 10.1039/D2RA01781D
- 15. M. Mahdavi, M. S. Shirazi, R. Taherkhani, M. Saeedi, E. Alipour, F. H. Moghadam, A. Moradi, H. Nadri, S. Emami, L. Firoozpour, A. Shafiee, A. Foroumadi, Eur. J. Med. Chem. **2014**, 82, 308–313. **DOI:** 10.1016/j.ejmech.2014.05.054
- 16. A. P. Keche, G. D. Hatnapure, R. H. Tale, A. H. Rodge, S. S. Birajdar, V. M. Kamble, Bioorg. Med. Chem. Lett. 2012, 22, 3445-3448. DOI: 10.1016/j.bmcl.2012.03.092
- 17. Z. Zhong, R. Xing, S. Liu, L. Wang, S. Cai, P. Li, Carbohydr. Res. 2008, 343, 566–570. DOI: 10.1016/j.carres.2007.11.024
- 18. S. Saeed, N. Rashid, P. G. Jones, M. Ali, R. Hussain, Eur. J. Med. Chem. 2010, 45, 1323-1331.
 - DOI: 10.1016/j.ejmech.2009.12.016
- 19. K. Ekoue-Kovi, K. Yearick, D. P. Iwaniuk, J. K. Natarajan, J. Alumasa, A. C. de Dios, P. D. Roepe, C. Wolf, Bioorg. Med. Chem. 2009, 17, 270-283. DOI: 10.1016/j.bmc.2008.11.009
- 20. D. Sriram, P. Yogeeswari, K. Madhu, Bioorg. Med. Chem. Lett. 2006, 16, 876-878. DOI: 10.1016/j.bmcl.2005.11.004
- 21. J. F. Strauss III, G. A. FitzGerald, in: J. F. Strauss III, R. L. Barbieri (Ed.), Yen and Jaffe's Reproductive Endocrinology, Elsevier, 2019, pp. 75-114.
 - DOI: 10.1016/B978-0-323-47912-7.00004-4
- 22. N. A. Sharif, N. Odani-Kawabata, F. Lu, L. Pinchuk, Exp. Eye Res. 2023, 229, 109415. DOI: 10.1016/j.exer.2023.109415
- 23. J. Wang, H. Chen, L. Zhuo, Y. Guo, X. Wang, L. Chen, F.

- Zheng, *J. Infect. Chemother.* **2023**, 29, 843–848. **DOI:** 10.1016/j.jiac.2023.05.004
- C. Palmieri, A. Musson, C. Harper-Wynne, D. Wheatley, G. Bertelli, I. R. Macpherson, M. Nathan, E. McDowall, A. Bhojwani, M. Verrill, J. Eva, C. Doody, R. Chowdhury, *Br. J. Cancer.* 2023, *129*, 852–860. DOI: 10.1038/s41416-023-02352-5
- A. Duminuco, A. Mosquera-Orgueira, A. Nardo, F. Di Raimondo, G. A. Palumbo, *Cancer Rep.* **2023**, *6*, e1881.
 DOI: 10.1002/cnr2.1881
- M. Weatherburn, Anal. Chem. 1967, 39, 971–974.
 DOI: 10.1021/ac60252a045
- S. Yaseen, M. K. Rauf, S. Zaib, A. Badshah, M. N. Tahir, M. I. Ali, Imtiaz-Ud-Din, M. Shahid, J. Iqbal, *Inorganica Chim. Acta* 2016, 443, 69–77. DOI: 10.1016/j.ica.2015.12.027
- M. A. S. Aslam, S. U. Mahmood, M. Shahid, A. Saeed, J. Iqbal, *Eur. J. Med. Chem.* 2011, 46, 5473–5479.
 DOI: 10.1016/j.ejmech.2011.09.009
- A. Saeed, S. U. Mahmood, M. Rafiq, Z. Ashraf, F. Jabeen, S. Y. Seo, *Chem. Biol. Drug Des.* **2016**, *87*, 434–443.
 DOI: 10.1111/cbdd.12675
- S. U. Mahmood, Y. Nazir, A. Saeed, Q. Abbas, Z. Ashraf, *ChemistrySelect.* 2020, 5, 5387–5390.

DOI: 10.1002/slct.202000429

- S. Zaib, R. Munir, M. T. Younas, N. Kausar, A. Ibrar, S. Aqsa,
 I. Khan, *Molecules*. 2021, 26, 6573.
 DOI: 10.3390/molecules26216573
- A. Balasubramanian, K. Ponnuraj, J. Mol. Biol. 2010, 400, 274–283. DOI: 10.1016/j.jmb.2010.05.009
- 33. D. Seeliger, B. L. De Groot, *J. Comput. Aided Mol. Des.* **2010**, 24, 417–422. **DOI:** 10.1007/s10822-010-9352-6
- 34. R. B. Jacob, T. Andersen, O. M. McDougal, *PLoS Comput. Biol.* **2012**, *8*, e1002499. **DOI:** 10.1371/journal.pcbi.1002499
- 35. A. Kumar, S. Kumar, S. Jain, P. Kumar, R. Goyal, *Med. Chem. Res.* **2013**, *22*, 5431–5441. **DOI:** 10.1007/s00044-013-0496-5
- 36. W. L. DeLano, Protein Crystallogr. 2002, 40, 82–92. https://mozart.gmb.bio.br/uploads/6/4/3/6/64362047/ pymol.pdf#page=44
- D. Santra, S. Maiti, Struct. Chem. 2022, 33, 1755–1769.
 DOI: 10.1007/s11224-022-02022-x
- A. Daina, O. Michielin, V. Zoete, Sci. Rep. 2017, 7, 42717.
 DOI: 10.1038/srep42717
- A. Ahmed, A. Saeed, O. M. Ali, Z. M. El-Bahy, P. A. Channar, A. Khurshid, A. Tehzeeb, Z. Ashraf, H. Raza, A. Ul-Hamid, M. Hassan, *Molecules*. 2021, 26, 7150.
 DOI: 10.3390/molecules26237150

Povzetek

Helicobacter pylori je Gram-negativna bakterija, ki je odgovorna za prebavne težave, vključno s kroničnim gastritisom in potencialno življenjsko ogrožujočim stanjem, kot je rak prebavil. Inhibicija encimov ureaz se je razkrila kot obetavna strategija za obvladovanje tovrstnih težav. Sintetizirali smo set *N*-aciltiosečnin 4a–j, ki vsebujejo ciklopentilno skupino, jih karakterizirali in določili njihovo sposobnost inhibiranja encima ureaze. Vse preiskovane spojine so izkazale inhibitorno aktivnost proti ureazi, celo večjo kot standardna spojina tiosečnina (IC₅₀ vrednost 23.00 ± 0.03 μM). Spojini 4a in 4b sta izkazali najvišjo inhibitorno učinkovitost z IC₅₀ vrednostima 2.21 ± 0.62 in 3.92 ± 0.59 μM. Ti dve spojini sta torej približno $10 \times$ oz. $6 \times$ boljša inhibitorja kot standardna spojina. Študije molekulskega sidranja so razkrile ključne interakcije med ligandom in aktivnim mestom. Simulacije molekulske dinamike in ADME študije so pokazale visoko stabilnost kompleksa ligand-protein in obnašanje, ki je ustrezno za zdravilne učinkovine, kar vse nakazuje na potencialno uporabnost našega pristopa pri razvoju novih poti pri zdravljenju gastritisa.



Except when otherwise noted, articles in this journal are published under the terms and conditions of the Creative Commons Attribution 4.0 International License